Jandl, J. H., Engle, L. K., & Allen, D. W. (1960) *J. Clin. Invest. 39*, 1818-1836.
Kunze, K. L., & Ortiz de Montellano, P. R. (1983) *J. Am. Chem. Soc. 105*, 1380-1381.
Mansuy, D., Battioni, J.-J., Dupre, D., & Sartori, E. (1982a) *J. Am. Chem. Soc. 104*, 6159-6161.
Mansuy, D., Battioni, P., Mahy, J.-P., & Gillet, G. (1982b) *Biochem. Biophys. Res. Commun. 106*, 30-36.
Ortiz de Montellano, P. R., & Kunze, K. L. (1981) *J. Am. Chem. Soc. 103*, 6534-6536.
Ortiz de Montellano, P. R., Kunze, K. L., & Augusto, O. (1982) *J. Am. Chem. Soc. 104*, 3545.
Ortiz de Montellano, P. R., & Kerr, D. E. (1983) *J. Biol. Chem. 258*, 10558-10563.
Ringe, D., Petsko, G. A., Kerr, D. E., & Ortiz de Montellano, P. R. (1984) *Biochemistry 23*, 2-4.
Rostorfer, H. H., & Cormier, M. J. (1957) *Arch. Biochem. Biophys. 71*, 235-249.
Saito, S., & Itano, H. A. (1981) *Proc. Natl. Acad. Sci. U.S.A. 78*, 5508-5512.

^1H and ^{31}P Relaxation Rate Studies of the Interaction of Phosphoenolpyruvate and Its Analogues with Avian Phosphoenolpyruvate Carboxykinase†

Thomas H. Duffy‡ and Thomas Nowak*

Program in Biochemistry and Biophysics, Department of Chemistry, University of Notre Dame, Notre Dame, Indiana 46556
Received April 3, 1984

ABSTRACT: The interactions of the substrate phosphoenolpyruvate and the substrate analogues (*Z*)-phosphoenol-α-ketobutyrate and (*E*)-phosphoenol-α-ketobutyrate with the enzyme–Mn complex of chicken liver phosphoenolpyruvate carboxykinase have been investigated by ^1H and by ^{31}P nuclear relaxation rate studies. Studies of the ^1H and the ^{31}P relaxation rates of the ligands in the binary Mn–ligand complexes show that these ligands interact with the metal ion via the phosphate group but not through the carboxylate. An inner sphere coordination complex is formed but the metal–ligand complex is not in the most extended conformation. In the relaxation rate studies of the ligands in the presence of the enzyme, conditions were adjusted so that all of the Mn^{2+} that was added resided in the ternary enzyme–Mn–ligand complex. The ^1H relaxation rates for each of the three ligands were measured at 100 and at 300 MHz. In each case the normalized paramagnetic effects showed that $1/(pT_{2p})$ was greater than $1/(pT_{1p})$. A frequency dependence of the $1/(pT_{1p})$ and $1/(pT_{2p})$ values was also measured. The correlation time, τ_c, for the Mn–^1H interaction was calculated from the frequency dependence of $1/(pT_{1p})$ assuming a maximal frequency dependence of τ_c and assuming no frequency dependence of τ_c and from the T_{1M}/T_{2M} ratios at each frequency. The τ_c values for all of the complexes, calculated at 100 MHz, varied from approximately 0.3 to 2.0 ns. These values were used to calculate the Mn–^1H distances in each of the ternary complexes. The relaxation rates of ^{31}P were also measured. The values of $1/(pT_{2p})$ were more than 1 order of magnitude larger than the respective values for $1/(pT_{1p})$ of ^1H and of ^{31}P for each ligand. A frequency dispersion, measured at 40.5 and at 121.5 MHz, was also observed for the $1/(pT_{1p})$ values. A calculation of the Mn–P distances shows that phosphoenolpyruvate forms an outer sphere complex with the bound Mn^{2+} ($r = 7.44 \pm 0.52$ Å). The structures of the ternary complexes with the *Z* and the *E* analogues ($r = 3.74 \pm 0.15$ Å and $r = 4.79 \pm 0.34$ Å, respectively, where *r* is the Mn–P distance) demonstrate that these inhibitors bind differently to the enzyme than does the substrate. The exchange rate of phosphoenolpyruvate ($k_{off} = 2.2 \times 10^4$ s^{-1}), measured from a temperature dependence of T_{2p}, is several orders of magnitude greater than the turnover number (30 s^{-1}) for the reaction. The activation energy for substrate exchange, 13 kcal/mol, suggests that this ligand exchange process is not a rate-determining step. These structural and kinetic results lead to a refinement of the proposed mechanism of this reaction and a clarification of the role of the Mn^{2+} activator.

Phosphoenolpyruvate carboxykinase (EC 4.1.1.32) catalyzes the reversible carboxylation of P-enolpyruvate[1] with a concomitant transfer of the phosphoryl group to a nucleotide acceptor, either IDP or GDP:

P-enolpyruvate + CO_2 + IDP (GDP) $\overset{Mn^{2+}}{\rightleftharpoons}$ oxalacetate + ITP (GTP)

The avian liver enzyme, which is mitochondrial in location, has been shown to require a divalent metal ion for activity, and Mn^{2+} gives optimal activity when used as the activator (Hebda & Nowak, 1982b). Kinetic, electron paramagnetic resonance, and proton relaxation rate studies have demonstrated a specific site on the enzyme for this cation, and the results have suggested that this metal is important in the

† This research was supported in part from research grants from the National Institutes of Health (AM 17049 and AM 00486) and a Grant-in-Aid from Miles Laboratories, Elkhart, IN. The support for the 300-MHz NMR spectrometer was provided by the General Medical Sciences Division of NIH and the Department of Chemistry, University of Notre Dame. T.N. is a Research Career Development Awardee of the National Institutes of Health (AM 00486).

‡ Work performed in partial fulfillment of the requirements for the degree of Doctor of Philosphy in Chemistry at the University of Notre Dame. Present address: Department of Biochemistry, Scripps Clinic and Research Foundation, La Jolla, CA.

[1] Abbreviations: P-enolpyruvate, phosphoenolpyruvate; PEB, phosphoenolbutyrate; FID, free-induction decay; Tris-HCl, tris(hydroxymethyl)aminomethane hydrochloride.

0006-2960/85/0424-1152$01.50/0

activation of the substrate P-enolpyruvate for phosphoryl transfer. On the basis of the available data, it has been postulated that the enzyme-bound Mn^{2+} activates the phosphoryl group of P-enolpyruvate for attack by IDP via the formation of an inner sphere Mn–phosphate complex (Hebda & Nowak, 1982b).

The role of the divalent cation activator has been investigated in other phosphoryl transferring enzymes. For instance, ^1H NMR studies (James & Cohn, 1974) demonstrated that the Mn^{2+} to pyruvate–proton distance (8.2 Å), for the K^+ form of the pyruvate kinase–Mn–pyruvate complex, was too large to accommodate a structure with direct Mn^{2+} coordination to pyruvate. These results were consistent with studies performed with ^{13}C NMR (Fung et al., 1973). An analogue of P-enolpyruvate, α-[(dihydroxyphosphinyl)methyl]acrylate, was found to bind through the phosphinyl group to the enzyme-bound Mn^{2+} (James & Cohn, 1974). Inner sphere complexes were determined with phosphoglycolate (Nowak & Mildvan, 1972) and with fluorophosphate (Nowak, 1978), products of pyruvate kinase catalyzed phosphorylation reactions of ATP. With Co^{2+} as a paramagnetic probe, the metal–phosphorus distance with P-enolpyruvate was calculated to be too far for a first coordination sphere complex (Melamud & Mildvan, 1975). Such results reflect the difficulty and suggest caution in the interpretation of experiments performed with a variety of analogues for a specific enzyme. Villafranca et al. (1980) showed that the distances of the α-, β-, and γ-phosphate groups of ATP to the bound Mn^{2+} on glutamine synthetase are 6.5, 6.8, and 5.9 Å, respectively. The bound metal apparently activates the phosphoryl group through an outer sphere complex. That complex is in contrast to the inner sphere Mn^{2+} complex of ATP reported for protein kinase (Granot et al., 1979). The Mn^{2+}–phosphorus distances of 3.0, 3.0, and 2.9 Å were determined for the α-, β-, and γ-phosphorus atoms of ATP, respectively (Granot et al., 1979). Li et al. (1979) had shown that the enzyme-bound metal of phosphoribosylpyrophosphate synthetase, which catalyzes a pyrophosphoryl transfer reaction, forms an outer sphere complex with the phosphoryl group of ribose 5-phosphate. A value of 3.8 Å was determined for the Mn^{2+}–γ-phosphorus distance of the nucleotide at the elongation site of RNA polymerase (Bean et al., 1977). It was suggested either that a distorted inner sphere metal–phosphate complexes existed or that the complex existed as a 20% inner, 80% outer sphere complex. It appears no *a priori* general conclusions may be drawn as to the nature of the divalent metal activator in phosphoryl transferring enzymes.

Detailed information of the role of the enzyme-bound Mn^{2+} in the formation of the substrate complex has not been reported with the enzyme P-enolpyruvate carboxykinase. This paper reports the results of nuclear relaxation rate studies with the enzyme P-enolpyruvate carboxykinase from avian liver. These studies were conducted with the substrate P-enolpyruvate and its structural analogues (*Z*)-PEB and (*E*)-PEB. These structural analogues of the substrate have previously been shown to be stereoselective competitive inhibitors with respect to P-enolpyruvate for the avian liver P-enolpyruvate catalyzed reaction but they do not elicit catalytic activity (Duffy et al., 1982).

Materials and Methods

P-enolpyruvate, IDP, ADP, and NADH were purchased from Sigma. P-enolpyruvate carboxykinase was purified from chicken liver as previously described (Hebda & Nowak, 1982a) with some modification. The calcium phosphate adsorption fractionation was replaced by column chromatography using DEAE-Bio-Gel A (no prior preparation of resin needed). The enzyme (1200 units, 4500 mg of protein) was loaded onto the anion exchange column (2.5 × 40 cm) at pH 8.0 in 5 mM potassium phosphate buffer. The column was washed with 400 mL of 5 mM potassium phosphate buffer, pH 8.0. Approximately 160 units of activity eluted with this wash. Enzyme was eluted with 5 mM potassium phosphate buffer, pH 7.0 (700 units, 475 mg of protein). The enzyme was then loaded without any additional treatment to an Affi-Gel Blue column (Bio-Rad) (2.5 × 10 cm) (1.5 mL/min). This column replaces the Blue Dextran column described by Hebda & Nowak (1982a). Pure P-enolpyruvate carboxykinase (65 mg, sp act. 7.1 units/mg) was eluted from the column with 2 mM IDP (1.5 mL/min). Lactate dehydrogenase, malate dehydrogenase, and pyruvate kinase were purchased from Boehringer-Mannheim Corp. (*Z*)-PEB and (*E*)-PEB were synthesized (Duffy et al., 1982) and were made metal free by passing them through a Chelex-100 column followed by lyophilization. Concentrations of P-enolpyruvate, (*Z*)-PEB, and (*E*)-PEB were measured by using the coupled pyruvate kinase–lactate dehydrogenase assay and limiting amounts of these substrates. The Mn^{2+} concentrations were determined by atomic absorption spectroscopy on a Varian Model AS-775 spectrometer. The enzyme that was used for the NMR experiments was first passed through a Bio-Rad P-6DG (1.1 × 25 cm) column having a 2-cm layer of Chelex-100 on the top. The column was preequilibrated with 0.065 M Tris-HCl buffer, pD 7.4, in D_2O for proton experiments and in H_2O for phosphorus experiments. The enzyme was concentrated in a Minicon B-15 concentrator. The enzyme was rediluted in buffer in D_2O 2–3 times and reconcentrated when the enzyme was to be used in proton experiments. The enzyme concentration was determined by its extinction coefficient ($\epsilon_{280}^{1\%}$ = 16.5), and a M_r of 72000 was used (Hebda & Nowak, 1982a). The specific activity of the enzyme (25 °C) was determined by measuring the carboxylation of P-enolpyruvate to yield oxalacetate with the MDH-coupled assay (Lee et al., 1981). The specific activity is defined as units of enzymatic activity per milligram of protein, and 1 unit is the amount of enzyme that catalyzes the formation of 1 μmol of product/min under experimental conditions. Enzyme with a specific activity of greater than 6.0 was used for the experiments. When necessary, 20 mM dithiothreitol was included with the enzyme for some experiments.

The relaxation rate experiments were performed on a Varian XL-100-15 spectrometer equipped with a TTI pulse system and Nicolet 1080 computer and on a Nicolet NTC 300 spectrometer with a 239A pulse system and 1180E computer. The T_1 measurements were made by the inversion recovery method (180°–τ–90°) (Vold et al., 1968; Allerhand et al., 1971) in the absence and in the presence of Mn^{2+}. For T_1 measurements, multiple scans were accumulated, at each τ value; the number of scans depended upon the signal-to-noise ratio of the particular experiments.

The T_1 was calculated from the raw data by the use of the Block equations where the magnetization (M_z), measured as the peak height, is equal to $M_0(1 - 2e^{-\tau/T_1})$, where M_0 is the peak height at equilibrium and τ is the delay time. The data are linearized, and a plot of ln $(M_\infty - M_t)$ vs. τ gives a slope of $-1/T_1$.

The T_2 values were estimated from the line widths of the resonance signals with the equation

$$1/T_2 = \pi(\nu_{1/2} - B)$$

where $\nu_{1/2}$ is the spectral line width at half-height in hertz and B is the artificial line broadening due to the exponential

multiplication of the FID prior to Fourier transformation of the spectrum. The value of B was usually 0.5 Hz. The T_2 values of the protons measured at 100 MHz were obtained from continuous-wave spectra obtained under slow-sweep conditions at a 100-Hz sweep width.

The ^1H relaxation rates at 100 MHz were measured from ^{31}P-decoupled spectra. The samples were run in 5-mm sample tubes with a final volume of 0.45–0.50 mL. The ^{31}P relaxation rates were obtained from ^1H-decoupled spectra. These samples were run in either 12- (on Varian XL-100) or 10-mm (Nicolet 300) sample tubes in a final volume of 2.5 or 3.0 mL. Unless mentioned otherwise, the temperature was monitored at 21 ± 1 °C.

All of the relaxation rate experiments (^1H and ^{31}P) were performed under analogous experimental conditions. Solutions were prepared in 65 mM Tris-HCl buffer, pD = 7.4, which contained 0.10 M KCl in D_2O. In the absence of enzyme, the concentration of ligand was approximately 100 mM for each of the experiments. The exact concentration was determined independently. The $1/T_1$ and $1/T_2$ values were measured as a function of increasing concentrations of $MnCl_2$. Four or more concentrations of Mn^{2+} were used for each experiment. The experiments performed in the presence of enzyme were devised to maximize the distribution of Mn^{2+} into the ternary enzyme–Mn–ligand complex. For the measurements of the ^1H relaxation rates, the enzyme concentration that was used was between 100 and 125 μM; the ligand concentration was anywhere from 41 to 131 mM. The Mn^{2+} concentration was varied from 0 to 81 μM; the exact values that were used were dependent upon the specific experimental conditions. For ^{31}P relaxation measurements the enzyme concentration was between 100 and 150 μM. The ligand concentration was anywhere from 33 to 53 mM and the Mn^{2+} was varied from 0 to 23 μM, depending upon the specific experimental conditions. In all of these experiments, the observed $1/T_1$ values increased by a factor of 2–15 upon the addition of increasing amounts of Mn^{2+}. The extent of the change in $1/T_1$ and in $1/T_2$ varied depending upon the experiment performed and upon experimental conditions. For each experiment that was performed, the distribution of Mn^{2+} was calculated on the basis of known dissociation constants for each complex (Duffy et al., 1982; Hebda & Nowak, 1981a). The calculations were performed with the program used to fit the proton relaxation rate titration experiments by using the dissociation constants that gave a "best fit" to the data (Duffy et al., 1982). In each experiment performed in the presence of enzyme, >98% of the Mn^{2+} was calculated to be in the ternary enzyme–Mn–ligand complex. In order to further verify the results of these calculations, several ^1H and ^{31}P experiments were performed at either two ligand concentrations or at two enzyme concentrations. The normalized relaxation rates were virtually identical.

The relaxation rates, $1/T_1$ and $1/T_2$, were plotted as a function of Mn^{2+} concentration. The paramagnetic contribution to the relaxation rates, $1/T_{1p}$ and $1/T_{2p}$ were calculated as the difference in relaxation rates due to Mn^{2+}. These values were normalized by the factor p, where $p = [Mn^{2+}]/[\text{ligand}]$, to yield values of $1/(pT_{1p})$ and $1/(pT_{2p})$. The normalized relaxation rates were assumed to be in fast-exchange domain for initial analysis, thus $1/(pT_{1p}) = 1/T_{1M}$ and $1/(pT_{2p}) = 1/T_{2M}$.

The correlation time, τ_c, for the electron–nuclear interaction was calculated for each of the binary and ternary complexes measured. For the binary complexes, τ_c was assumed to be τ_r, the rotational correlation time. For the binary complexes studied, this value increases approximately 80% from the τ_r for $Mn(H_2O)_6$ (3×10^{-11} s) (Bloembergen & Morgan, 1955) when the $Mn(H_2O)_5$–ligand complex is formed (Nowak, 1978). A value of 5.38×10^{-11} s was calculated for τ_c for the binary complexes on the basis of the increase in molecular weight of the complex.

Two separate methods were used to determine τ_c in the ternary complexes. Both of these methods utilized the dipolar forms of the Solomon–Bloembergen equations (Solomon, 1955; Solomon & Bloembergen, 1956):

$$\frac{1}{T_1} = \frac{2S(S+1)\gamma^2 g^2 \beta^2}{15r^6}\left(\frac{3\tau_c}{1+\omega_I^2\tau_c^2} + \frac{7\tau_c}{1+\omega_s^2\tau_c^2}\right) \quad (1)$$

$$\frac{1}{T_{2M}} = \frac{S(S+1)\gamma^2 g^2 \beta^2}{15r^6}\left(4\tau_c + \frac{3\tau_c}{1+\omega_I^2\tau_c^2} + \frac{13\tau_c}{1+\omega_s^2\tau_c^2}\right) \quad (2)$$

where S is the electron-spin quantum number, γ is the nuclear magnetogyric ratio, r is the ion–nuclear distances, g is the electronic "g" factor, β is the Bohr magneton, and ω_I and ω_s are the Larmor angular precession frequencies for the nuclear and electron spins, respectively. A frequency dependence of $1/T_{1M}$ for the nucleus measured was used to calculate τ_c. Assuming τ_c is frequency independent, eq 3

$$\frac{T_{1M}(\nu_2)}{T_{1M}(\nu_1)} = \frac{1+\omega_{I(\nu_2)}^2\tau_c^2}{1+\omega_{I(\nu_1)}^2\tau_c^2} \quad (3)$$

was used to calculate τ_c. Assuming a maximal frequency dependence of τ_c, eq 4 was used to calculate τ_c at ν_1 and ν_2.

$$\frac{T_{1M}(\nu_2)}{T_{1M}(\nu_1)} = \frac{1+\omega_{I(\nu_2)}^2(\nu_2/\nu_1)^2\tau_c^2}{1(\nu_2/\nu_1)^2+\omega_{I(\nu_1)}^2\tau_c^2} \quad (4)$$

The second method to calculate τ_c utilized the $1/T_{2M}$ to $1/T_{1M}$ ratio. Assuming only dipolar contributions of Mn^{2+} to the relaxation rates, τ_c can be calculated from the following relationship:

$$\tau_c = \left(\frac{6-7F}{4\omega_I^2 F}\right)^{1/2} \quad (5)$$

where F is the T_{1M}/T_{2M} ratio.

The longitudinal relaxation rates of the nuclei of a complexed ligand ($1/T_{1M}$) may be used in the Solomon–Bloembergen equations to calculate interatomic distances between the paramagnetic ion and the magnetic nuclei from the dipolar correlation time, τ_c. As noted earlier, the equation is restricted by the limits of fast exchange ($pT_{1p} = T_{1M}$). For Mn–^1H interactions in a 1:1 complex, the simplified form of eq 1 is

$$r\ (\text{Å}) = 812[T_{1M}f(\tau_c)]^{1/6} \quad (6)$$

and for Mn–^{31}P, the equation simplies to

$$r\ (\text{Å}) = 601[T_{1M}f(\tau_c)]^{1/6} \quad (7)$$

The term $f(\tau_c)$ is the correlation function, which is defined as

$$f(\tau_c) = \frac{3\tau_c}{1+\omega_I^2\tau_c^2} + \frac{7\tau_c}{1+\omega_s^2\tau_c^2} \quad (8)$$

More detailed descriptions of the treatment of these data have been reviewed elsewhere [i.e., Nowak (1981) and Mildvan & Gupta (1978)].

A temperature dependence of the ^{31}P relaxation rates of P-enolpyruvate in the ternary complex was performed at 121.5 MHz. One sample contained enzyme, buffer, KCl, and substrate and the second sample contained identical solutions and included Mn^{2+}. Detailed conditions are given in the figure

Table I: ^1H and ^{31}P Relaxation Rates of Binary Mn–Phosphate Complexes and Calculated Mn^{2+}–Nuclear Distances

ligand	nucleus	$1/(pT_{1p})$ (s^{-1})	$1/(pT_{2p})$ (s^{-1})	r (Å)[a]
P-enolpyruvate	$^1H_{(cis)}$	$(6.0 \pm 0.1) \times 10^3$	$(8.6 \pm 0.5) \times 10^3$	4.44 ± 0.1
	$^1H_{(trans)}$	$(3.1 \pm 0.1) \times 10^3$	$(3.3 \pm 0.1) \times 10^3$	4.96 ± 0.1
	^{31}P	$(1.2 \pm 0.1) \times 10^4$	$(1.8 \pm 0.2) \times 10^6$	2.93 ± 0.1
(*Z*)-PEB	$^1H_{(methyl)}$	$(5.3 \pm 0.6) \times 10^3$	$(10.0 \pm 1.0) \times 10^3$	4.53 ± 0.1
	$^1H_{(vinyl)}$	$(10.2 \pm 0.6) \times 10^3$	$(17.0 \pm 3.0) \times 10^3$	4.07 ± 0.3
	^{31}P	$(1.6 \pm 0.1) \times 10^4$	$(1.7 \pm 0.2) \times 10^6$	2.80 ± 0.1
(*E*)-PEB	$^1H_{(methyl)}$	$(2.3 \pm 0.6) \times 10^3$	$(11.7 \pm 1.3) \times 10^3$	5.21 ± 0.2
	$^1H_{(vinyl)}$	$(7.8 \pm 0.3) \times 10^3$	$(10.0 \pm 3.1) \times 10^3$	4.25 ± 0.2

[a] Calculated using $\tau_c = 5.38 \times 10^{-11}$ s.

legend. Differences in relaxation rates between the Mn^{2+}-containing complex and the diamagnetic control were calculated to give values for the paramagnetic contribution to the relaxation rates. The temperature was varied by passing cooled nitrogen over a thermostated heating element before it arrived at the sample zone. The temperature of the sample within the probe was measured directly by means of a thermocouple.

Results

Binary Mn–Ligand Complexes. The effects of Mn^{2+} on the relaxation rates of the protons of P-enolpyruvate and of the analogues (*E*)-PEB and (*Z*)-PEB were measured in the binary Mn–ligand complexes at 100 MHz. The ^1H spectra were ^{31}P decoupled. Plots of ln $(M_\infty - M_t)$ vs. τ were linear. The concentration of P-enolpyruvate was 80 mM, and the concentrations of (*Z*)-PEB and (*E*)-PEB were 131 and 128 mM, respectively. The Mn^{2+} concentrations varied from 6 to 76 μM in these experiments. The relaxation rates were normalized for the concentrations of ligand and for the concentration of Mn^{2+}, and the results are summarized in Table I. Table I also summarizes the results of the effect of Mn^{2+} on the relaxation rates of the phosphorus nuclei of P-enolpyruvate and of the analogue (*Z*)-PEB, which were measured at 40.5 MHz. The ^{31}P experiments were performed at 53 and 50 mM ligand, respectively, and Mn^{2+} was varied up to a concentration of 4.4 μM.

Mn^{2+}–Nuclei Distances in Binary Complexes. Table I summarizes the results of Mn–proton distances calculated for the binary Mn–ligand complexes with eq 6. A value of 5.38×10^{-11} s was calculated as a correlation time for the binary complexes. This value is based upon the assumptions that a 1:1 complex is formed and that $\tau_c = \tau_r$ and τ_r is directly proportional to the molecular weight of the complex. The Mn–phosphorus distances were also calculated for the binary complexes with eq 7, and these results are also summarized in Table I. Distances of approximately 2.8 ± 0.1 Å between the Mn^{2+} and the phosphorus of P-enolpyruvate and of (*Z*)-PEB were calculated. The Mn–phosphorus distance in (*E*)-PEB was assumed to be similar to its diastereomer, (*Z*)-PEB. These distances are consistent with inner sphere coordination complexes. The values calculated are in agreement with those measured for other Mn–phosphate complexes measured under similar conditions [i.e., Mildvan et al. (1973) and Nowak (1978)], indicating that the structure of these complexes is similar to those for other binary Mn–phosphate complexes.

^1H and ^{31}P Relaxation Rates of Ligands in Ternary Enzyme–Mn–Ligand Complexes. The effects of P-enolpyruvate carboxykinase bound Mn^{2+} on the proton relaxation rates of P-enolpyruvate and the inhibitors (*Z*)-PEB and (*E*)-PEB were measured at 100 and at 300 MHz. The results of one such experiment are shown in Figure 1. The $1/T_1$ values increased by a factor of 2–10 upon the addition of up to 80 μM Mn^{2+}. The increase depended upon the specific ligand used. The data

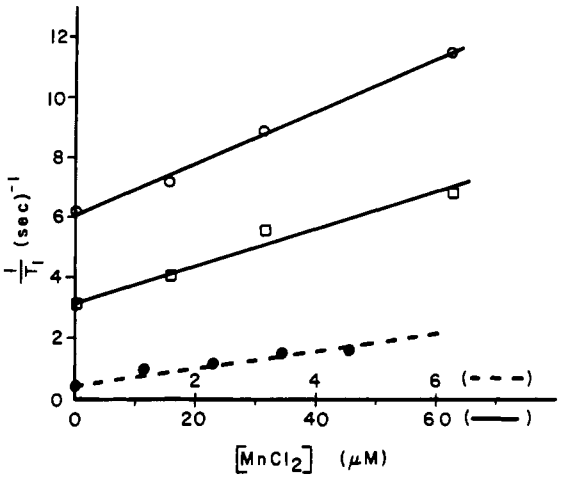

FIGURE 1: Measured $1/T_1$ values of the nuclei of (*E*)-PEB in the ternary PEPCK–Mn–(*E*)-PEB complex. The $1/T_1$ values of the upfield (methyl) protons (○) and the downfield (vinyl) proton (□) of (*E*)-PEB were measured as a function of Mn^{2+} concentration in the presence of PEPCK. This experiment was performed at 129 mM (*E*)-PEB and 131 μM PEPCK in 65 mM Tris-HCl and 100 mM KCl, pD 7.4 in D_2O, in a final volume of 0.45 mL. The measurements were performed at 100 MHz, and the sample was ^{31}P decoupled. The 90° pulse width was 26 μs. The delay time for each experiment was at least 10 times longer than the null point for each determination. The number of acquisitions was 4 for the experiment in the absence of Mn^{2+} and was progressively increased as the concentration of Mn^{2+} increased. The $1/T_1$ for ^{31}P was measured (●) from ^1H-decoupled spectra. This experiment was performed at 40.5 MHz with 53 mM (*E*)-PEB and 121 μM PEPCK in 3.0 mL under conditions otherwise identical with the experiments performed as described above. The 90° pulse width was 40 μs. The temperature was maintained at 21 ± 1 °C with precooled N_2 gas. Additional details were as described under Materials and Methods.

Table II: ^1H Relaxation Rates of Ligands in Ternary Enzyme–Mn–Ligand Complexes

ligand	proton(s)	$1/(pT_{1p})$ (s^{-1})	$1/(pT_{2p})$ (s^{-1})
P-enol-pyruvate	cis	$(1.1 \pm 0.2) \times 10^4$[a]	$(1.4 \pm 0.2) \times 10^4$[a]
		$(2.5 \pm 0.4) \times 10^3$[b]	$(6.0 \pm 0.5) \times 10^3$[b]
	trans	$(0.51 \pm 0.30) \times 10^4$[a]	$(0.78 \pm 0.24) \times 10^4$[a]
		$(1.1 \pm 0.1) \times 10^3$[b]	$(3.0 \pm 0.4) \times 10^3$[b]
(*Z*)-PEB	methyl	$(0.97 \pm 0.07) \times 10^4$[a]	$(2.3 \pm 0.9) \times 10^4$[a]
		$(3.4 \pm 0.1) \times 10^3$[b]	$(11.0 \pm 2.0) \times 10^3$[b]
	vinyl	$(1.3 \pm 0.1) \times 10^4$[a]	$(4.5 \pm 0.3) \times 10^4$[a]
		$(7.3 \pm 0.5) \times 10^3$[b]	$(21.0 \pm 4.0) \times 10^3$[b]
(*E*)-PEB	methyl	$(0.72 \pm 0.04) \times 10^4$[a]	$(2.3 \pm 0.3) \times 10^4$[a]
		$(0.94 \pm 0.10) \times 10^3$[b]	$(5.6 \pm 0.2) \times 10^3$[b]
	vinyl	$(1.05 \pm 0.15) \times 10^4$[a]	$(4.6 \pm 0.2) \times 10^4$[a]
		$(4.2 \pm 0.4) \times 10^3$[b]	$(17 \blacksquare 2) \times 10^3$[b]

[a] Measured at 100 MHz. [b] Measured at 300 MHz.

were normalized by the value p and summarized in Table II. The distribution of Mn^{2+} was calculated for each experiment, and virtually all of the Mn^{2+} (>98%) was calculated to be in the ternary enzyme–Mn–ligand complex in each case. The experiment that contained P-enolpyruvate was repeated at approximately 35% greater enzyme concentration. The ex-

Table III: ^{31}P Relaxation Rates of Ligands in Ternary Enzyme–Mn–Ligand Complexes

ligand	$1/(pT_{1p})$ (s^{-1})	$1/(pT_{2p})$ (s^{-1})
P-enolpyruvate	$(1.0 \pm 0.1) \times 10^{3}$ [a]	$(4.5 \pm 0.7) \times 10^{4}$ [a]
	$(0.29 \pm 0.05) \times 10^{3}$ [b]	$(2.2 \pm 0.3) \times 10^{4}$ [b]
(*Z*)-PEB	$(3.4 \pm 0.1) \times 10^{4}$ [a]	$(9.0 \pm 0.5) \times 10^{5}$ [a]
	$(2.4 \pm 0.4) \times 10^{4}$ [b]	$(11 \pm 1) \times 10^{5}$ [b]
(*E*)-PEB	$(1.6 \pm 0.2) \times 10^{4}$ [a]	$(6.3 \pm 0.2) \times 10^{5}$ [a]
	$(0.36 \pm 0.04) \times 10^{4}$ [b]	$(1.7 \pm 0.2) \times 10^{5}$ [b]

[a] Measured at 40.5 MHz. [b] Measured at 121.5 MHz.

periment that contained (*Z*)-PEB was repeated at approximately 50% lower ligand concentration. The normalized relaxation rates from these experiments were nearly identical with those values measured for the original experiments. The normalized $1/T_{1p}$ and $1/T_{2p}$ values, measured in the presence of the enzyme at 100 MHz, are enhanced over the values measured for the binary Mn–ligand complexes.

The effects of enzyme-bound Mn^{2+} on the ^{31}P relaxation rates for the three ligands were measured at 40.5 and at 121.5 MHz. The $1/T_1$ values increased by a factor of 4–20 as Mn^{2+} was added up to a concentration of 7.2 μM. The data are summarized in Table III. The normalized relaxation rates measured at 40.5 MHz for the complexes containing P-enolpyruvate and (*E*)-PEB are less than the respective values measured for the binary Mn–ligand complexes.

Correlation Times for the Mn^{2+}–Nuclear Interactions in Various Ternary P-enolpyruvate Carboxykinase–Mn–Ligand Complexes. In order to use the relaxation rate data in Tables II and III to calculate the Mn^{2+}–nuclear distance r from eq 6 and 7, the ligands must be in fast exchange [$1/(pT_{1p}) = 1/T_{1M}$] and the correlation time, τ_c, must be known. It has previously been demonstrated (Nowak, 1981) that when $1/(pT_{2p})$ values are substantially larger than $1/(pT_{1p})$ values, $1/(pT_{1p})$ is a measure of relaxation ($1/T_{1M}$) and is in the rapid exchange domain. Since $1/(pT_{2p})$ values, measured for ^{31}P for each of the three ligands studied (Table III), are much larger than the $1/(pT_{1p})$ and $1/(pT_{2p})$ values for the protons measured in the same complex (Table II), these latter values reflect rapid exchange [$1/(pT_{1p}) = 1/T_{1M}$; $1/(pT_{2p}) = 1/T_{2M}$.[2] Furthermore, $1/(pT_{1p}) = 1/T_{1M}$ for ^{31}P with each of the three ligands at both frequencies. The correlation times for the Mn–^1H interactions for each complex can be calculated from the $1/T_{1M}$ values measured at 100 and at 300 MHz. Analogous calculations were performed with $1/T_{1M}$ values measured for ^{31}P at 40.5 and at 121.5 MHz (Table IV). These calculations for the correlation time were performed assuming no frequency dependence of τ_c (eq 3). Since τ_c values are approximately the values anticipated if τ_c is the electron relaxation time (τ_s) for Mn^{2+}, τ_c may be frequency dependent (Bloembergen & Morgan, 1961). The values for τ_c were also calculated assuming a maximal frequency dependence (eq 4). The results of these calculations are also tabulated in Table IV. Correlation times were also calculated from the T_{1M}/T_{2M} ratios for each nucleus measured at each frequency with eq 5. The results of these calculations are summarized in Table IV. The abnormally long values for τ_c calculated from T_{1M}/T_{2M} measurements of ^{31}P indicate that the T_{2M} values contain scalar contributions to the relaxation.[3] These values of τ_c were not used in our calculations. The frequency dispersion of $1/(pT_{1p})$ observed for ^1H and for ^{31}P and the agreement of values for τ_c that were calculated confirm that our calculations for the distribution of Mn^{2+} and our assumptions that $1/(pT_{1p}) = 1/T_{1M}$ are correct.

Table IV: Correlation Times (τ_c) for Ternary E–Mn–Ligand Complexes

complex	nucleus measd	ν_I (MHz)	τ_c ($\times 10^9$ s) from ω_I [a]	from ω_I [b]	from T_{1M}/T_{2M}
E–Mn–P-enolpyruvate	cis ^1H	100	0.38	0.52	0.60
		300	3.4		0.72
	trans ^1H	100	0.39	0.53	0.99
		300	3.5		0.66
	^{31}P	40.5	0.80	2.2	32.0
		121.5	7.2		14.0
E–Mn–(*Z*)-PEB	methyl ^1H	100	0.30	0.38	2.1
		300	2.7		0.94
	vinyl ^1H	100	0.23	0.25	2.1
		300	2.1		0.85
	^{31}P	40.5	0.50	0.89	24.0
		121.5	4.5		11.0
E–Mn–(*E*)-PEB	methyl ^1H	100	0.51	0.72	2.8
		300	4.6		1.4
	vinyl ^1H	100	0.28	0.34	3.5
		300	2.5		1.1
	^{31}P	40.5	0.91	2.6	30.0
		121.5	8.2		11.0

[a] Assuming a maximal frequency dependence of τ_s. [b] Assuming no frequency dependence of τ_c.

Mn^{2+}–Nuclei Distances in Ternary Enzyme–Mn–Ligand Complexes. The correlation times, calculated from the relaxation rates that were measured for each nucleus, were used to calculate the correlation functions [$f(\tau_c)$] (eq 8) at each frequency. The values for $f(\tau_c)$ (Table V) and the values measured for $1/(pT_{1p})$ (Tables II and III) were used to calculate the Mn^{2+}–nuclear distances, r. These calculations were performed with the simplified Solomon–Boembergen equations, eq 6 and 7. The values for r are summarized in Table V. The error levels indicated in Table V are obtained by taking extreme values for T_{1M} and for $f(\tau_c)$ to calculate a value for r. The values calculated for the Mn–^1H distances for each of the ternary complexes investigated are too great to suggest inner sphere coordination complexes. The Mn–^{31}P distances that were measured in the ternary complexes are also summarized in Table V. In each complex that was studied, the distances between the enzyme-bound Mn^{2+} and the phosphorus atom of the ligand are too great for an inner sphere complex. These results confirm the deductions drawn from the ^1H measurements. The Mn–P distance to the substrate P-enolpyruvate is substantially greater than the Mn–P distance for the two substrate analogues. The distances measured are consistent with second sphere complexes where a ligand such as water can intervene between the phosphate of the ligand and the enzyme-bound Mn^{2+}.

Temperature Effects of ^{31}P Relaxation Rates in the Enzyme–Mn–P-enolpyruvate Complex. In an attempt to confirm that the nuclei of P-enolpyruvate in the ternary complex may be in fast exchange, a temperature dependence of the ^{31}P relaxation rates was measured. A plot of the relaxation rate

[2] One reviewer has suggested that the value of $1/(pT_{2p})$ for ^{31}P of P-enolpyruvate in the E–Mn–P-enolpyruvate complex may be influenced by a contribution from the binary Mn–P-enolpyruvate complex. If 1% of the Mn^{2+} was in the binary complex, the maximum contribution based on the analysis of data in Tables I and III, a substantial effect on $1/(pT_{2p})$ for ^{31}P but not for ^1H is possible. A 1% distribution is impossible to measure or calculate with any reliability. If 1% binary complex is present, the inequality of pT_{2p} and pT_{1p} to show fast exchange is not rigorous in our analysis with P-enolpyruvate. The results of the temperature effects on $1/(pT_{2p})$ are consistent with our assumptions however (vide infra).

[3] If a contribution to $1/(pT_{2p})$ for ^{31}P of P-enolpyruvate by the binary complex is present, this statement may not be true for this ternary complex.

Table V: Correlation Functions [$f(\tau_c)$] for E-Mn-Ligand Complexes and Mn-Nuclear Distances

ligand	nucleus	ν_I (MHz)	$f(\tau_c)$ ($\times 10^9$ s) from ω_I[a]	from ω_I[b]	from T_{1M}/T_{2M}	r (Å)
P-enolpyruvate	cis ^{1}H	100	1.1	1.4	1.6	5.73 ± 0.13
		300	0.24	0.80	0.76	6.27 ± 0.53
	trans ^{1}H	100	1.1	1.4	2.1	6.61 ± 0.26
		300	0.24	0.80	0.78	7.22 ± 0.62
	^{31}P	40.5	2.3	5.0		7.38 ± 0.48
		121.5	0.69	5.0		7.50 ± 0.57
(*Z*)-PEB	methyl ^{1}H	100	0.86	1.1	2.3	5.82 ± 0.38
		300	0.38	0.75	0.68	6.05 ± 0.28
	vinyl ^{1}H	100	0.68	0.73	2.3	5.36 ± 0.48
		300	0.38	0.61	0.72	5.28 ± 0.22
	^{31}P	40.5	1.5	2.5		3.73 ± 0.16
		121.5	1.1	1.8		3.75 ± 0.15
(*E*)-PEB	methyl ^{1}H	100	1.4	1.8	2.1	6.32 ± 0.19
		300	0.18	0.76	0.52	7.12 ± 0.64
	vinyl ^{1}H	100	0.81	0.98	1.8	5.61 ± 0.30
		300	0.32	0.72	0.62	5.70 ± 0.30
	^{31}P	40.5	2.6	5.4		4.72 ± 0.29
		121.5	0.61	1.6		4.86 ± 0.39

[a] Calculated from τ_c obtained by assuming a maximal frequency dependence. [b] Calculated from τ_c assuming no frequency dependence.

effects as a function of temperature is shown in Figure 2. The $1/T_{1p}$ exhibited no substantial change over the temperature range measured. An increase in $1/T_{2p}$ upon increase in temperature was noted. The diamagnetic control showed essentially no change in $1/T_1$ or $1/T_2$ over the range observed. The negative slope for $1/T_{2p}$, seen in Figure 2, is characteristic of slow chemical exchange. The exchange rate (k_{off}) and the energy of activation for this process may be calculated. Since the $1/(pT_{2p})$ is the exchange rate or k_{off} ($1/\tau_m = 2.2 \times 10^4$ s^{-1}) for the ligand P-enolpyruvate and if we assume simple complex formation, $K_d = k_{off}/k_{on}$, a value for k_{on} was calculated. The K_d value (0.25×10^{-6} M) used in this calculation was obtained from proton relaxation rate studies (Duffy et al., 1982). A value for k_{on} at 20 °C of 8.88×10^{10} M^{-1} s^{-1} was calculated. This value is consistent with a diffusion controlled reaction. A value of 13 kcal/mol was obtained for the energy of activation of P-enolpyruvate departure from the ternary enzyme–Mn–P-enolpyruvate complex.

Discussion

The effects of the Mn^{2+} on the ^{1}H and the ^{31}P relaxation rates of the nuclei of P-enolpyruvate, of (*E*)-PEB, and of (*Z*)-PEB were measured in the binary Mn–ligand complexes at 100 MHz for protons and at 40.5 MHz for phosphorus. The results from these experiments were used to calculate the Mn–nuclear distances, r, in these complexes. The equation used to calculate r (eq 1) is restricted by the limits of fast exchange ($pT_{1p} = T_{1M}$). For the proton relaxation rates $1/(pT_{2p})$ values are consistently larger than $1/(pT_{1p})$ values. A comparison of $1/(pT_{2p})$ of the phosphorus nuclei with the $1/(pT_{1p})$ of the phosphorus nuclei and with $1/(pT_{1p})$ and $1/(pT_{2p})$ of the proton nuclei showed that the $1/(pT_{2p})$ of phosphorus is 2 orders of magnitude greater than the $1/(pT_{1p})$ values. Two conclusions may be drawn from these results. First, $1/(pT_{2p})$ values for the phosphorus nuclei are either exchange rates of the ligand from Mn^{2+} ($1/\tau_m$) or are limits to this process. Second, the $1/(pT_{1p})$ value of phosphorus and $1/(pT_{1p})$ and $1/(pT_{2p})$ values for protons are dominated by relaxation and not by chemical exchange ($pT_{1p} = T_{1M}$; $1/\tau_M \geq 1.7 \times 10^6$ s^{-1}). The large $1/(pT_{2p})$ values for the phosphorus nuclei indicate a substantial scalar contribution for the Mn^{2+}. With relaxation data in Table I and the value of 5.38, $\times 10^{-11}$ s for τ_c, Mn–nuclei distances were calculated from the Solomon–Bloembergen equation.

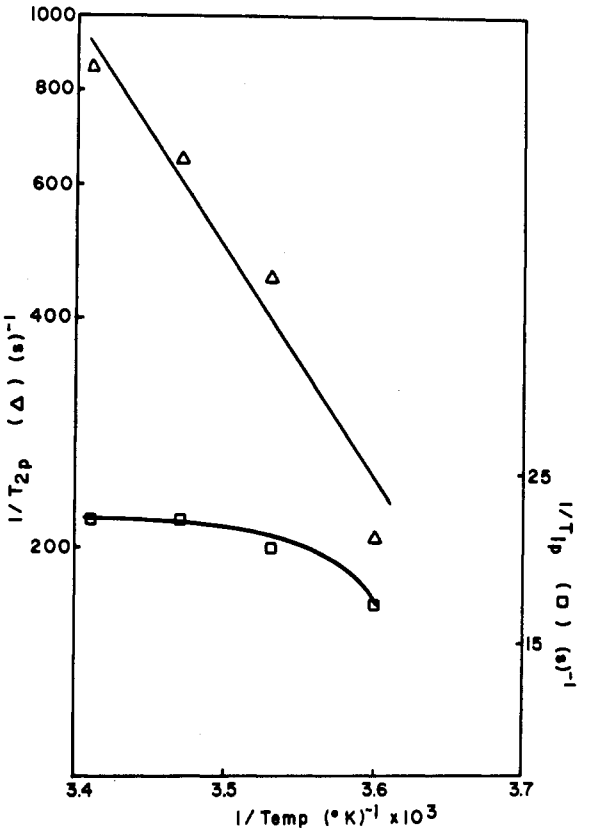

FIGURE 2: Temperature dependence of the paramagnetic effects on $1/T_1$ and $1/T_2$ of ^{31}P in the ternary PEPCK–Mn–P-enolpyruvate complex. The results for $1/T_{1p}$ (□) and $1/T_{2p}$ (Δ) are plotted vs. reciprocal temperature. The sample in 3.2 mL contained 50 mM PEP, 100 μM PEPCK, 100 mM KCl, and 28 μM $MnCl_2$ in 65 mM Tris-HCl, pD 7.4. The paramagnetic effect was calculated by subtraction of a diamagnetic control that was prepared in an identical fashion but did not contain $MnCl_2$. The relaxation rates were measured as described under Materials and Methods. This experiment was performed at 121.5 MHz.

P-enolpyruvate and its analogues contain two possible liganding groups for the Mn^{2+}: the carboxyl and the phosphate groups. The distances calculated between Mn^{2+} and the protons of the ligands (Table I) in the binary complexes are inconsistent with carboxyl coordination but are consistent with phosphoryl coordination. The Mn–P distances in these binary complexes place the phosphoryl group of the ligand within the

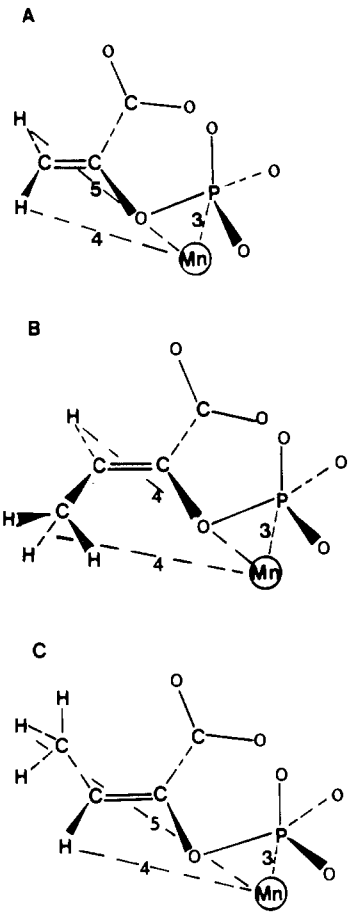

FIGURE 3: Geometry of the binary Mn–ligand complexes. The structures of the (A) Mn–P-enolpyruvate, (B) Mn–(*Z*)-PEB, and (C) Mn–(*E*)-PEB complexes are shown on the basis of the distances calculated for the Mn^{2+}–phosphorus and Mn–proton atoms in the respective complexes. The numbers are the Mn^{2+}–atom distances in angstroms, rounded off and taken from Table I.

first coordination sphere of the Mn^{2+}. The structures of these complexes are similar to other Mn–phosphate complexes, measured under similar conditions [i.e., Mildvan et al. (1973) and Nowak (1978)]. These compounds show either monodentate or bidentate coordination of the Mn^{2+} to phosphate. The three binary Mn–phosphate complexes all appear to be planar and similar in structure (Figure 3).

The effects of P-enolpyruvate carboxykinase bound Mn^{2+} on the ^1H and ^{31}P relaxation rates of P-enolpyruvate, (*Z*)-PEB, and (*E*)-PEB are shown in Tables II and III. The experimental conditions used for these experiments (concentration of enzyme and ligand) were adjusted so that the Mn^{2+} that was added was essentially all (>98%) in the ternary complex. These experiments were designed on the basis of calculations using binding parameters previously measured (Duffy et al., 1982). The results of these calculations were verified by the observation of a frequency dependence of the longitudinal relaxation rates and by the observation that an increase in enzyme concentration or a decrease in ligand concentration does not substantially alter the normalized relaxation rates. A comparison of the $1/(pT_{2p})$ values of the ^{31}P nucleus of each of the ligands with the $1/(pT_{1p})$ value and the $1/(pT_{1p})$ and $1/(pT_{2p})$ values of the ^1H nuclei of the same ligand demonstrate that the latter relaxation rates are in the rapid exchange domain (see footnote 2). The positive temperature dependence of $1/(pT_{2p})$ for ^{31}P of P-enolpyruvate supports this argument. The substrate P-enolpyruvate exchanges from the ternary complex at least 1 order of magnitude more slowly ($k_{off} \sim 3 \times 10^4\ s^{-1}$) than do the competitive inhibitors (*Z*)-PEB ($k_{off} \sim 100 \times 10^4\ s^{-1}$) and (*E*)-PEB ($k_{off} \geq 40 \times 10^4\ s^{-1}$). (*Z*)-PEB binds to the enzyme–Mn complex nearly 2 orders of magnitude less tightly than does P-enolpyruvate. The exchange rate of (*Z*)-PEB has the same activation barrier (13.5 kcal/mol) (data not shown) as that for P-enolpyruvate. The ligands P-enolpyruvate and (*E*)-PEB bind with equal affinity however (Duffy et al., 1982). The differences between exchange rates for these ligands and the contrast between k_{off} values for P-enolpyruvate and (*E*)-PEB suggest that the modes of binding and the types of interactions between enzyme–Mn and the ligands differ. Steric effects with the PEB analogues distort the ligand binding at the catalytic site. The structures of the ligands in the respective ternary ligand complexes substantiate those conclusions.

In order to calculate the electron–nuclear distance and hence to obtain structural data for the ternary complexes from these experiments, the correlation time is required. Three separate calculations were performed to obtain τ_c values (Table IV). The values for τ_c are in reasonable agreement. A comparison of τ_c values at 100 and at 300 MHz, calculated assuming a maximal frequency dependence, with τ_c calculated from T_{1M}/T_{2M} at the same frequency show that the values at 100 MHz are lower and the values at 300 MHz are higher than the values calculated from T_{1M}/T_{2M} at the same frequency. These results suggest that τ_c may not be maximally frequency dependent at these higher frequencies. The values for τ_c calculated from T_{1M}/T_{2M} from ^{31}P measurements were all uniformly longer than any of the other values calculated. Although the values for $1/(pT_{2p}) < 1/T_{2M}$, the large values for $1/(pT_{2p})$ may be due to a substantial hyperfine interaction for T_{2M}. These values were not used to calculate $f(\tau_c)$ nor to calculate values of r. The values for $f(\tau_c)$ were in reasonable agreement regardless of the ligand measured or the nucleus measured (Table V). These values for τ_c for various P-enolpyruvate carboxykinase–Mn–ligand complexes are approximately the same as the values measured for other ternary complexes that have been investigated with this enzyme (Makinen & Nowak, 1983; Lee & Nowak, 1984).

The values for r calculated for ^1H and for ^{31}P for each ligand were used to construct structural models for the respective ternary complexes (Figure 4). From the Mn–P distances calculated, each of the ligands formed an outer sphere complex with the bound Mn^{2+}. However, the structures of the complexes with the substrate P-enolpyruvate and the inhibitors (*Z*)-PEB and (*E*)-PEB differ substantially.

In the ternary enzyme–Mn–P-enolpyruvate complex, the Mn may be situated either above or below the plane of the substrate molecule. During catalysis, the substrate CO_2 approaches P-enolpyruvate from above the plane or the *si* face to add stereospecifically to the C-3 atom of the substrate (Rose et al., 1969; S.-H. Hwang and T. Nowak, unpublished observations). Kinetic studies suggest that the Mn^{2+} does not influence the interaction of CO_2 with the enzyme (Hebda & Nowak, 1982a). We therefore postulate that the Mn^{2+} is below the plane of P-enolpyruvate, exposed to the *re* face of the substrate. The distance from the Mn^{2+} to the phosphorus atom is sufficiently large (7.4 ± 0.5 Å) to allow a molecule of water or some other residue to intervene between the phosphoryl group and the bound Mn^{2+}. The nature of this intervening ligand has not yet been determined. From the value of r (7.44 Å) calculated for the Mn^{2+} to phosphorus distance in the ternary enzyme–Mn–P-enolpyruvate complex and the estimated correlation time [$\tau_c \sim (1.5 \pm 0.6) \times 10^{-9}$ s], $1/T_{2M}$ was calculated ignoring any scalar interaction. The

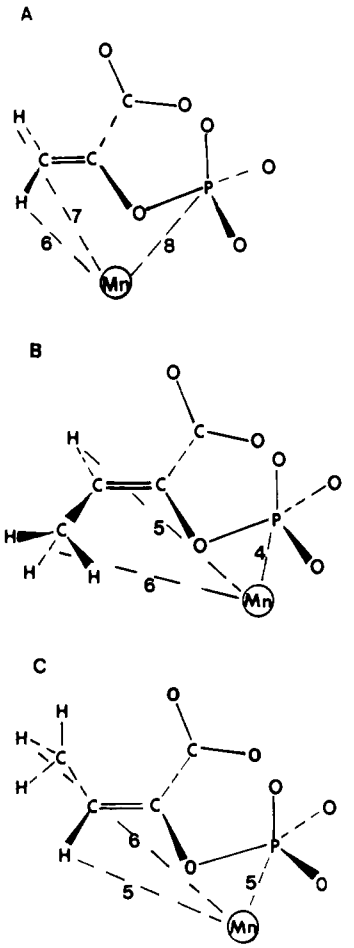

FIGURE 4: Geometry of the ternary PEPCK–Mn–ligand complexes. The structures of the enzyme–Mn complex that contains (A) P-enolpyruvate, (B) (*Z*)-PEB, and (C) (*E*)-PEB are shown. These structures are based on the Mn^{2+}–phosphorus and Mn–proton distances calculated for the respective complexes. The numbers in the figure are rounded-off values for the Mn^{2+}–atom distances, in angstroms, taken from Table V.

calculated value (1.4×10^3 s^{-1}) is 1 order of magnitude smaller than the measured $1/(pT_{2p})$, which is a lower limit to $1/T_{2M}$.[4] This difference in $1/T_{2M}$ suggests that there is a substantial electron delocalization between the enzyme-bound Mn^{2+} and the phosphorus atom of the substrate. This effect is present although the complex is outer sphere. This observation suggests that the bound metal ion may activate the phosphorus atom of the substrate toward reaction even though a direct coordination sphere complex is apparently not formed. Such an observation has also been made with the nucleotide substrate with this enzyme (Lee & Nowak, 1984).

The models drawn for the complexes formed with (*Z*)-PEB and (*E*)-PEB indicate that the C-3 position of the ligand, the potential site of carboxylation, is displaced horizontally away from the phosphoryl transfer site by using the location of the Mn^{2+} as a fixed point. The model (Figure 4) indicates steric crowding at the catalytic site. A possible consequence of steric crowding is that CO_2 is unable to bind or unable to bind correctly at the catalytic site. A proton relaxation rate titration of the enzyme–Mn–P-enolpyruvate complex with HCO_3^- shows an increase in observed enhancement from 6 to 7 indicating that CO_2 binds to the ternary complex and causes a perturbation about the bound Mn^{2+} (Hebda & Nowak, 1982b). A similar perturbation was observed with both (*Z*)-PEB and (*E*)-PEB as ligands (data not shown). These results suggest that the lack of substrate activity with these two analogues was not due to the inability of CO_2 to bind. Perhaps the steric effects that force the inhibitors closer to the Mn^{2+} in the vertical plane of the catalytic site misalign the phosphate group with respect to the β-phosphate of the nucleotide substrate to preclude the phosphoryl transfer reaction, hence catalysis.

[4] This analysis assumes no contribution to $1/(pT_{2p})$ by the binary complex.

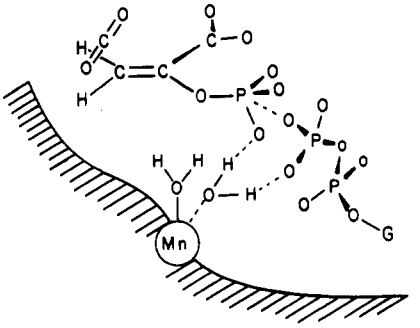

FIGURE 5: Proposed mechanism for the P-enolpyruvate carboxykinase catalyzed reaction. The orientation of the substrates with respect to enzyme-bound Mn^{2+} is shown. This model is based on the data reported here and from other studies (Lee & Nowak, 1984; Hebda & Nowak, 1982b; S.-H. Hwang and T. Nowak, unpublished observations). The second cation, which also takes part in the catalytic reaction as the metal–nucleotide complex (Lee et al., 1981), is deleted from the figure for purposes of simplicity. The exact location of this cation has not yet been determined, but it is thought to form a β,γ-bidentate complex with GTP.

From the temperature dependence of $1/T_{2p}$ for ^{31}P of P-enolpyruvate this value is determined to be the exchange rate of the substrate, $1/\tau_m = 4.5 \times 10^4$ s^{-1}. By using the dissociation constant for this complex, K_3 (0.25×10^{-6} M) (Duffy et al., 1982), and assuming a simple ligand exchange mechanism, the rate of formation of the ternary complex can be calculated ($k_{on} = 8.9 \times 10^{10}$ M^{-1} s^{-1}). This rapid rate constant suggests a diffusion-controlled reaction (Eigen & Hammes, 1963) and argues against a ligand substitution reaction of a divalent or trivalent anion that replaces a coordinated water molecule on Mn^{2+} [$k = 1.6 \times 10^9$ M^{-1} s^{-1} (Eigen & Hammes, 1963; Mildvan & Cohn, 1970; Nowak et al., 1973)]. The activation energy for P-enolpyruvate exchange, 13 kcal/mol, is lower than the activation energy of the carboxylation reaction [17.6 kcal/mol (Hebda & Nowak, 1982a)], suggesting that substrate departure is not rate limiting in the catalytic reaction. On the basis of the present structural and kinetic data, a revised mechanism for chicken liver P-enolpyruvate carboxykinase can be proposed. The outline for this proposed mechanism is shown in Figure 5. Not only does the substrate P-enolpyruvate form an outer sphere complex with the enzyme-bound Mn^{2+} but the nucleotide does so as well (Lee & Nowak, 1984). Optimal alignment of these substrates, apparently oriented by the bound Mn^{2+}, is required for enzymic catalysis.

ACKNOWLEDGMENTS

We are indebted to Donald Schifferl for his assistance with the NMR spectrometers.

Registry No. P-enolpyruvate, 138-08-9; (*Z*)-PEB, 31302-64-4; (*E*)-PEB, 31302-89-3; Mn, 7439-96-5; phosphoenolpyruvate carboxykinase, 9013-08-5.

REFERENCES

Allerhand, A., Doddrell, D., & Komoroski, R. (1971) *J. Chem. Phys. 55*, 189–197.

Bean, B. L., Koren, R., & Mildvan, A. S. (1977) *Biochemistry 16*, 3322–3333.
Bloembergen, N., & Morgan, L. (1961) *J. Chem. Phys. 34*, 842.
Duffy, T. H., Saz, H. J., & Nowak, T. (1982) *Biochemistry 21*, 132–139.
Dwek, R. A. (1973) *Nuclear Magnetic Resonance in Biochemistry*, Clarendon Press, Oxford.
Eigen, M., & Hammes, G. (1963) *Adv. Enzymol. Relat. Areas Mol. Biol. 25*, 1–25.
Granot, J., Armstrong, R. N., Kondo, H., Kaiser, E. T., & Mildvan, A. S. (1979) *Fed. Proc., Fed. Am. Soc. Exp. Biol. 38*, 315.
Hebda, C. A., & Nowak, T. (1982a) *J. Biol. Chem. 257*, 5503–5514.
Hebda, C. A., & Nowak, T. (1982b) *J. Biol. Chem. 257*, 5515–5522.
James, T. L. (1975) *Nuclear Magnetic Resonance in Biochemistry*, pp 177–209, Academic Press, New York.
James, T. L., & Cohn, M. (1974) *J. Biol. Chem. 249*, 3519–3526.
Lee, M.-H. (1983) Ph.D. Thesis, University of Notre Dame.
Lee, M.-H., & Nowak, T. (1984) *Biochemistry 23*, 6506–6513.
Li, H., Switzer, R. L., & Mildvan, A. S. (1979) *Arch. Biochem. Biophys. 193*, 1–13.
Makinen, A. L., & Nowak, T. (1983) *J. Biol. Chem. 258*, 11654–11662.
Melamud, E., & Mildvan, A. S. (1975) *J. Biol. Chem. 250*, 8193–8201.
Mildvan, A. S., & Cohn, H. (1970) *Adv. Enzymol. Relat. Areas Mol. Biol. 33*, 1–71.
Mildvan, A. S., & Nowak, T. (1973) *Ann. N.Y. Acad. Sci. 222*, 192–210.
Mildvan, A. S., & Gupta, R. K. (1978) *Methods Enzymol. 49*, 322–358.
Nowak, T. (1978) *Arch. Biochem. Biophy. 186*, 343–350.
Nowak, T. (1981) *Spectrosc. Biochem. 2*, 109–135.
Nowak, T., & Mildvan, A. S. (1972) *Biochemistry 11*, 2819–2828.
Nowak, T., Mildvan, A. S., & Kenyon, G. L. (1973) *Biochemistry 12*, 1690–1701.
Reuben, J., & Cohn, M. (1970) *J. Biol. Chem. 245*, 6539–6546.
Rose, I. A., O'Connell, E. L., Noce, P., Utter, M. F., Wood, H. G., Willard, J. M., Cooper, T. G., & Benziman, M. (1969) *J. Biol. Chem. 244*, 6130–6133.
Solomon, I. (1955) *Phys. Rev. 99*, 559–565.
Solomon, I., & Bloembergen, N. (1956) *J. Chem. Phys. 25*, 261–266.
Villafranca, J. J. (1980) *Dev. Biochem. 10*, 17–30.
Vold, R. L., Waugh, J. S., Klein, M. P., & Phelps, D. E. (1968) *J. Phys. Chem. 48*, 3831–3832.
Watson, D. G., & Kennard, O. (1973) *Acta Crystallogr., Sect. B 29*, 2358–2364.

Opposite Effects of Cofilin and Profilin from Porcine Brain on Rate of Exchange of Actin-Bound Adenosine 5′-Triphosphate†

Eisuke Nishida

Department of Biophysics and Biochemistry, Faculty of Science, University of Tokyo, Hongo, Tokyo 113, Japan
Received June 12, 1984

ABSTRACT: Cofilin, an actin-binding protein isolated from porcine brain that reacts with actin in a 1:1 molar ratio [Nishida, E., Maekawa, S., & Sakai, H. (1984) *Biochemistry 23*, 5307–5313], decreases the rate of exchange of ATP bound to G-actin with 1,N^6-ethenoadenosine 5′-triphosphate in solution. From analyses of the dependence of the exchange rate on the cofilin concentration under different KCl concentrations, dissociation constants (K_D) for the cofilin–actin binding at 0, 50, and 140 mM KCl were determined to be 0.12, 0.15, and 0.25 μM, respectively. In contrast to cofilin, profilin isolated from porcine brain increases the rate of exchange of G-actin-bound ATP, like *Acanthamoeba* profilin. The kinetic analyses gave K_D values for the profilin–actin binding of 1.1 and 1.5 μM, respectively, at 50 and 200 mM KCl.

Many actin-binding proteins that regulate the state of actin polymerization or higher order structures of actin have been isolated from various tissues and cells (Weeds, 1982; Craing & Pollard, 1982). We have been interested in the regulation of the microfilament system in mammalian tissues and isolated several G-actin-binding proteins from porcine brains by the use of DNase I–agarose affinity chromatography (Nishida et al., 1981; Maekawa et al., 1984).

Cofilin, one of such proteins, has complex effects on actin with the ability to bind to both G- and F-actin (Nishida et al., 1984b). It binds to actin filaments in a 1:1 molar ratio of cofilin to actin monomer in the filament, shortens the average length of the filament, and increases the steady-state concentration of monomeric actins to a limited extent.

It is well-known that G-actin contains 1 mol of bound ATP and that the bound ATP is exchangeable with ATP in solution (Kuehl & Gergely, 1969). Previously, two G-actin-binding proteins have been shown to affect the rate of exchange of actin-bound ATP. DNase I decreases the exchange rate (Mannherz et al., 1980; Hitchcock, 1980), while *Acantha-*

† This work was supported in part by Grants-in-Aid from the Ministry of Education, Science and Culture of Japan (57440004, 57380016, and 58780176).

0006-2960/85/0424-1160$01.50/0